Modeling and simulation of a torsion actuator made of nylon filament

Cite as: AIP Conference Proceedings **2411**, 090003 (2021); https://doi.org/10.1063/5.0067641
Published Online: 02 November 2021

Justín Murín, Juraj Paulech, Vladimír Goga, et al.

Modeling and Simulation of a Torsion Actuator Made of Nylon Filament

Justín Murín[1, a)], Juraj Paulech[1], Vladimír Goga[1], Juraj Hrabovský[1], Vladimír Kutiš[1], Roman Kmotorka[1] and Mehdi Aminbaghai[2]

[1] *Department of Applied Mechanics and Mechatronics*, *Institute of Automotive Mechatronics, FEI STU in Bratislava, Ilkovičova 3, 812 19 Bratislava, Slovakia*
[2] *Institute for Mechanics of Materials and Structures, Vienna University of Technology, Karlsplatz 13, A-1040 Vienna, Austria.*

[a)] Corresponding author: justin.murin@stuba.sk

Abstract: The actuator of the angle of rotation or torque is presented that consists of two identical prestressed polymer springs of negative thermal expansion coefficient and a perfectly rigid angled beam in the shape of an inverted letter T. A mathematical-physical model for thermoelastic linear and nonlinear analysis of the torsional actuator is compiled, the result of which are the values of the action angle of rotation and torque of the actuator. The action is achieved by heating the polymer springs with a negative thermal expansion. The results of semianalytical models that can be used for automatic actuator control were verified by numerical analysis using the finite element method. The proposed torsion actuator shows a relevant action already at low warming of the nylon springs.

1. INTRODUCTION

Polyethylene and nylon filaments which are commonly used as a fishing line [1], can be effectively used as an integral part of the mechatronic system, which is conditioned by the application of torsional stress to the fiber, which causes its deformation and subsequent change of placement fibrillar elements in the monofilament. In the literature, such a system is also called artificial muscle. From a practical point of view, this means that the polymer filament must be twisted into the shape of a spring using a controlled twisting process. Immediately after winding the spring, the adjacent threads are in contact and represent a prestressed tension spring, which limits shrinkage during activation, and therefore the threads must be separated by increasing the longitudinal load. When adjacent threads are in contact, due to insufficient applied load or excessive torsion, the thermal expansion of the muscle remains positive. When adjacent threads are not in contact due to the applied additional load, the thermal expansion of the muscle is negative and the muscle performs mechanical work as published in the most prestigious scientific journal "Science" in 2014 as a scientific discovery [1]. Recently, several researches around the world have been concerned with the characterization of such artificial muscles by experimental and computational methods, and their practical applications are being sought. In particular, it is a question of determining their mechanical and thermo-mechanical properties. In the article [2] a new polymeric artificial muscle based on a composite was prepared and characterized. The work [3] presents an artificial muscle made of nylon fishing line, which is used to convert thermal energy into electrical energy. The results of experimental research of thermo-mechanical properties of nylon muscle are published in the article [4]. The work [5] deals with the current state of research of macroscopic artificial muscles, which work on the basis of electro-thermal excitation. The work [6] presents an artificial muscle made of twisted nylon 6.6 fiber. This article presents an effective phenomenological constitutive model, which contains several physical properties of artificial muscle. Article [7] describes the mechanical behaviour of nylon drives and investigates the elasticity and strength of the nylon spring as a function of temperature. The work [8] presents a new

Applied Physics of Condensed Matter (APCOM 2021)
AIP Conf. Proc. 2411, 090003-1–090003-8; https://doi.org/10.1063/5.0067641
Published by AIP Publishing. 978-0-7354-4138-5/$30.00

structure of biomimetic nylon drive, which mimics the human muscle with the ability to change stiffness and tensile strength by adding additional fibers. The work [9] presents technical data on the production process of selected artificial muscle drives. The construction of a new artificial muscle to drive an artificial robotic arm and the results of its experimental research are described in [10]. The work [11] describes an artificial muscle replacement made of ionometric composite. Multiscale approaches are also used to model these structures [12]. Comparison of modeling results and experimental results showed excellent agreement. In the work [13] a new type of support system simulating the movement of the human body driven by muscle contractions is proposed. The main characteristic of the above references is that experimental methods are used for the research of artificial muscles in conjunction with analytical calculations according to phenomenological relationships. In our previous works [14, 15, 16, 17], the results of our team on the area of research and application of the nylon springs is presented.

The aim of this article is to present the development and research of a possible application of nylon artificial muscles in the form of a torsional actuator. Analytical mathematical models are compiled for the torque actuator, which contains mechanical and thermomechanical parameters obtained by measuring real nylon springs. By applying these models, it is possible to obtain the magnitude of the action torque as well as the rotation angle of the actuator for elasto-thermomechanical loading. The obtained characteristics of the actuator can be used in further research for automatic control and management of the action intervention.

2. ACTUATOR DESCRIPTION

The actuator of the angle of rotation or torque consists of two identical prestressed polymer springs and perfectly rigid angled beam in the shape of an inverted letter T. The parameters of the springs are (see Fig. 1 and Fig. 3): l_0 - initial length, k_m - spring constant obtained by measuring from tensile test, a - length of horizontal arm, b - length of vertical arm, F_p - prestressing compressive force of springs created by their production technology, k_T - temperature constant obtained by measuring thermal shortening of one spring loaded by respective tensile force F_m, or by calculation described in chapter 3. The angled T-beam is supported by a fixed joint at point P. At its end points D and C, the upper ends of the springs are fixed. The springs are then stretched at points A and B by an extension Δl_m to positions A' and B', in which they are fixed after extension. By heating the left or right spring by the temperature difference ΔT, the horizontal arms turn by an angle φ, and the point E is moved to the point E'. By turning the arms of the actuator, the corresponding torque can be developed by thermo-mechanical forces.

3. THERMOELASTIC ANALYSIS OF THE ACTUATOR

The aim of the thermoelastic analysis is to calculate the angle of rotation φ, the torque M_t, the coupling reactions at points A, B and P, as well as the displacement of point E. There are two ways to compile the necessary equations. For small angles of rotation φ, it can be assumed that points C and D move only vertically. This model is called linear (Fig. 1). In the second case, we will assume that the endpoints C and D of perfect rigid arms turn along a circle with radius a (Fig. 3). In this way, the springs are tilted from their original vertical position. This model is called nonlinear. Both mathematical models will be compiled and solved in the following chapters.

3.1 Linear Model of the Actuator

The linear model of the actuator is shown in its initial and deformed configurations in Fig. 1. Vertical extension of the springs by the selected value Δl_m creates a tensile force $F_m = F_p + k_m \Delta l_m$ in the springs (Fig. 2). The length of the stretched springs is $l_m = l_0 + \Delta l_m$. At points A and B, vertical reactions $A_m = B_m = F_m$ occur. By heating the left spring by ΔT, the point C is moved to the point C' by the value $\Delta l_{T1} = k_T \Delta T / 2$. By the same value, but in the opposite direction, the point D of the right spring is moved to the point D'. The horizontal displacement of the point E is $\Delta E = b \tan \varphi$. The thermal shortening of the left spring can also be expressed by the thermal force F_T and the effective tensile stiffness of the spring as $\Delta l_{T1} = F_T l_m / ES$, where ES is the axial stiffness of the replacement rod with effective cross section S and modulus of elasticity E.

Multiplying the right side of this expression by l_0 / l_0 and after appropriate mathematical adjustment, the thermal force can be expressed: $F_T = k_T \Delta T k_m \varepsilon / 2$, where $\varepsilon = l_0 / l_m$ is the ratio of the initial and extended length of the spring. The stiffness of the equivalent rod is equal to the spring constant: $k_m = ES / l_0 = \tan(\alpha_m)$, Fig. 2.

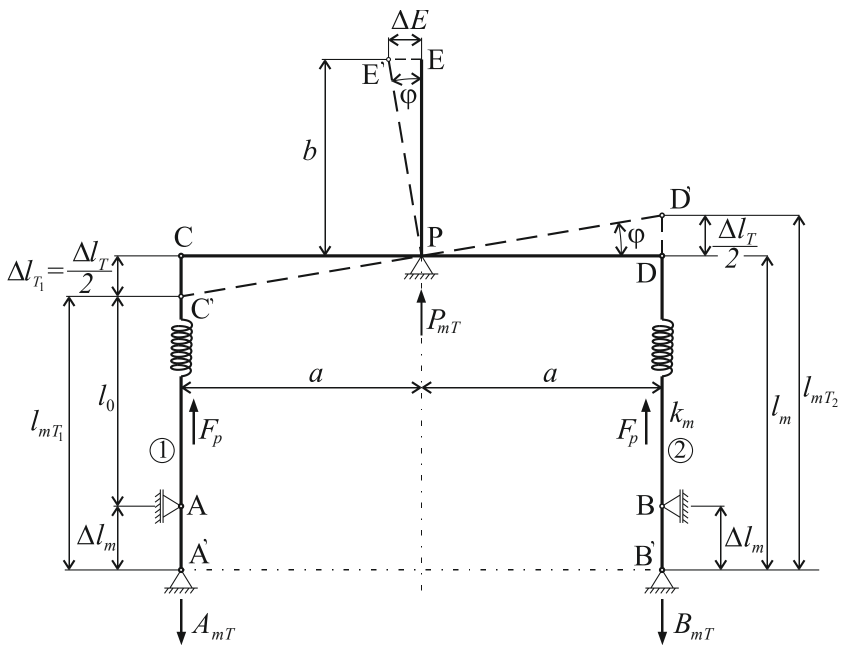

FIGURE 1. Linear model of the torsion actuator

The magnitude of the binding reactions is: $A_{mT} = B_{mT} = F_m + F_T$, $P_{mT} = A_{mT} + B_{mT}$. The resultant torsion moment that is caused by the thermal force is $M_{t\varepsilon} = 2F_T a$. If the thermal force is calculated with parameter $\varepsilon = 1$, then the resultant torsional moment is in Tables 2 - 4 marked by M_t. In this case, a heating of the spring length l_0 is assumed.

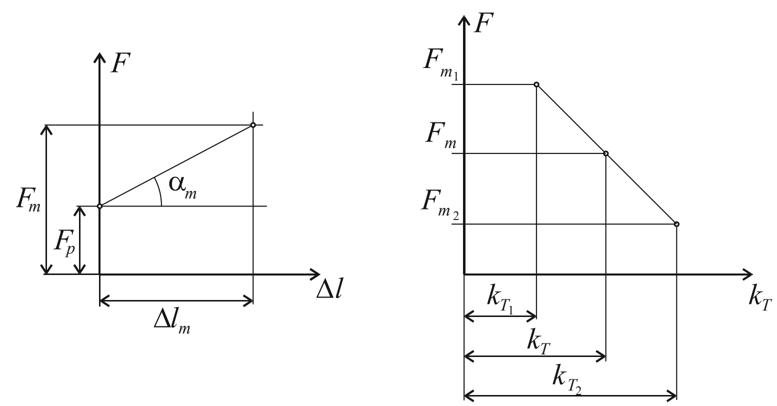

FIGURE 2. Measurement of the spring and thermal constants

3.2 Nonlinear Model of the Actuator

Figure 3 shows the deformed position of the actuator after the extension of the springs by Δl_m and the thermal shortening of the left spring $\Delta l_{T1} = k_T \Delta T/2$. The new length of the shortened spring is according to Fig. 3

$$l_{mT1} = l_m - \Delta l_{T1} = \sqrt[2]{\left(a(1-\cos\varphi)\right)^2 + (l_m - a\sin\varphi)^2}. \tag{1}$$

After the appropriate mathematical operations we get a nonlinear equation to calculate the unknown angle φ:

$$2a^2 + l_m^2 - 2a^2\cos\varphi - 2al_m\sin\varphi - (l_m - k_T\Delta T/2)^2 = 0. \tag{2}$$

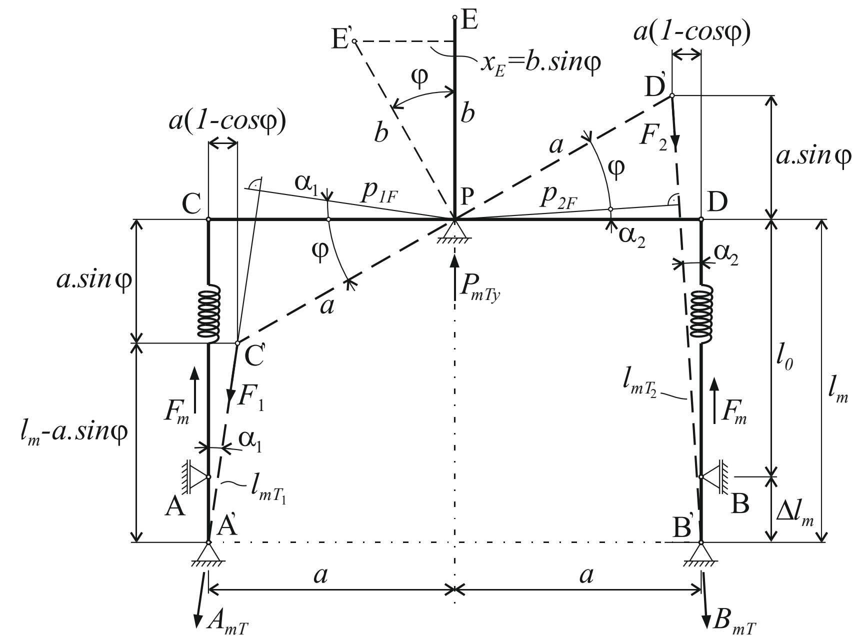

FIGURE 3. Nonlinear model of the torsion actuator

The solution of this equation can be performed e.g. commercial software MATHEMATICA [18]. Substituting the calculated real value of the angle φ into equation (1) it is possible to determine the deformed length of the left spring (1), and from equation (3) also the length of the right spring

$$l_{mT2} = l_m + \Delta l_{T1} = \sqrt[2]{\left(a(1-\cos\varphi)\right)^2 + (l_m + a\sin\varphi)^2}\,. \tag{3}$$

The resulting axial forces in the springs are

$$F_1 = (F_m + F_T)/\cos\alpha_1 = \left(F_m + \tfrac{k_m k_T \Delta T \varepsilon}{2}\right)/\cos\alpha_1\,,\;\; F_2 = (F_m + F_T)/\cos\alpha_2 = \left(F_m + \tfrac{k_m k_T \Delta T \varepsilon}{2}\right)/\cos\alpha_2, \tag{4}$$

where $F_T = k_m k_T \Delta T\varepsilon/2$ is the thermal force. Then $A_{mT} = F_1$, $B_{mT} = F_2$.
From the geometry of the deformed system in Fig. 3, the angles α_1 and α_2 in radians can be determined:

$$\alpha_1 = \mathrm{asin}\varphi\left(\frac{a(1-\cos\varphi)}{l_{mT1}}\right),\; \alpha_2 = \mathrm{asin}\varphi\left(\frac{a(1-\cos\varphi)}{l_{mT2}}\right). \tag{5}$$

The actuating torque of the actuator can be expressed in the form

$$M_{t\varepsilon} = (F_1 - F_m)p_{1F} + (F_2 - F_m)p_{2F}, \tag{6}$$

where $p_{1F} = a\cos(\varphi + \alpha_1)$ and $p_{2F} = a\cos(\varphi - \alpha_2)$ are the arms of the forces F_1 and F_2 to the pivot point P. If the thermal force is calculated with parameter $\varepsilon = 1$, then the resultant torsional moment is in Tables 2 - 4 is marked by M_t.The horizontal displacement of the point E is $x_E = b\sin\varphi$.

4. MEASUREMENT AND CALCULATION OF THE THERMAL CONSTANT OF THE NYLON SPRINGS

As is clear from the above actuator models, the temperature constant of the respective spring k_T must be measured. If no, it can be determined from the following experiment and method. The selected vertically oriented spring attached at its upper end is loaded at its lower end with a mass m (Fig. 4), which represents the tensile force $F_m = mg$, where g is the gravitational acceleration. As mentioned above, this force elongates the spring with the compressive prestressing force F_p and with an initial length l_0 by the value Δl_m. As a rule, this extension is primarily chosen, which is the same for both springs. Then the required force is $F_m = F_p + k_m \Delta l_m$.

By heating the elongated spring by the temperature difference ΔT, it is shortened by the value Δl_T. Then the temperature constant $k_T = \Delta l_T / \Delta T$. It is obvious that the spring constant of a given spring depends on its mechanical extension Δl_m, resp. on the magnitude of the force F_m that the thermomechanical force must overcome. In a system of several springs, the axial forces of the individual springs are mostly unknown, and therefore it was necessary to design the following experimental-computational model for determining the temperature constants. Assume the performance of two measurements of the shortening of an applied spring loaded by two different forces $F_{m1} > F_{m2}$, which are heated by the same temperature difference ΔT.

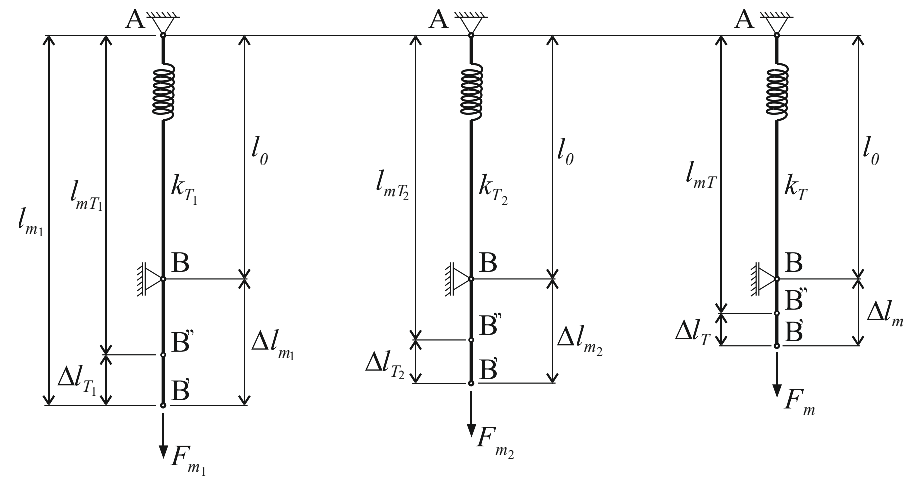

FIGURE 4. Measurement of the temperature constant of a selected spring

According to Fig. 4, the springs are shortened by the values $\Delta l_{T1} < \Delta l_{T2}$, where $\Delta l_{T1} = k_{T1} \Delta T$ and $\Delta l_{T2} = k_{T2} \Delta T$. We assume a linear relationship between the loading forces and the temperature constants according the diagram in Fig. 2. From this dependence it is possible to determine a new thermomechanical spring parameter λ, which applies to $F_m \in \langle F_{m2}, F_{m1} \rangle$:

$$\lambda = \tan\gamma = \frac{F_{m1}-F_{m2}}{k_{T2}-k_{T1}} = \frac{F_{m1}-F_m}{k_T-k_{T1}} = \frac{F_m-F_{m2}}{k_{T2}-k_T}\,. \tag{7}$$

Using this parameter, it is possible to determine the temperature constant for the selected elongation Δl_m, or the resulting force F_m

$$k_T = \frac{F_{m1}-F_m}{\lambda} + k_{T1} = \frac{F_m-F_2}{\lambda} + k_{T2}\,. \tag{8}$$

If the temperature constant was measured for F_{m1} resp. F_{m2}, then k_T is equal to k_{T1} resp. k_{T2}.

5. RESULTS OF SEMIANALYTICAL AND NUMERICAL THERMOELASTIC ANALYSIS OF TORSION ACTUATOR

An actuator with the following parameters was chosen for the semianalytical method (Fig. 1 and Fig. 3): l_0 = 105 mm, k_m = 0.212 N/mm, F_p = 2.1 N, a = 50 mm, b = 25 mm, g = 9.81 m/s^2. According to Chapter 3, measurements of the temperature constant were performed for 3 values of elongation of one spring: Δl_{m1} = 14.62 mm, Δl_{m2} = 9.99 mm, Δl_{m3} = 5.36 mm, corresponding to three loads - weights m_1 = 0.53 kg, m_2 = 0.43 kg, m_3 = 0.33 kg. When the spring warmed by ΔT =10°C, the temperature constants k_{T1} = 0.302 mm/°C, k_{T2} = 0.311mm/°C, k_{T3} = 0.322 mm/°C were measured [15]. It is clear from the above results that the temperature constant decreases with increasing elongation of the spring. As the measurement showed, these temperature constants are independent of the magnitude of the heating ΔT, but there was a slight dependence on the thermomechanical lifting of the respective mass. To verify the functionality of the procedure for calculating the temperature constant mentioned in Chapter 3, the temperature constant for the elongation of the spring Δl_m= 12 mm was determined. From equation (7) we get the temperature parameter of the spring λ = 98.82 N °C/mm and from relation (8) the temperature constant k_T = 0.307 mm/°C. Table 1 shows the results of the analytical thermoelastic analysis of both linear (L) and nonlinear (NL) models of the torsional actuator for left spring heating by ΔT = 10°C. The AT symbol indicates the type of analysis.

TABLE 1. Torsional actuator parameters.

AT	m [kg]	Δl_m [mm]	l_m [mm]	ε [-]	F_m[N]	Δl_{T1}[mm]	k_T[mm/°C]
L, NL	m_3 = 0.33	5.36	110.36	0.95	3.24	1.61	0.322
L, NL	m_2 = 0.43	9.99	114.99	0.91	4.22	1.55	0.311
L, NL	m_1 = 0.53	14.62	119.62	0.88	5.20	1.51	0.302
L, NL	m = 0.47	12.00	117.00	0.89	4.64	1.54	0.307

TABLE 2. Results of thermoelastic semianalytic analysis of the torsional actuator.

m/AT [kg]/-	φ [rad]	φ [°]	A_{mT} B_{mT} [N]	x_E [N]	P_{mT} [N]	l_{mT1} [mm]	l_{mT2} [mm]	F_T [N]	$M_{t\varepsilon}$ [Nmm]	M_t [Nmm]
0.33/L	0.032	1.84	-3.56	0.81	7.12	108.75	111.97	0.32	32.5	34.1
0.33/NL	0.032	1.84	-3.56	0.80	7.12	108.75	111.97	0.32	32.4	34.0
0.43/L	0.031	1.78	-4.52	0.78	9.04	113.43	116.54	0.30	30.1	32.9
0.43/NL	0.031	1.78	-4.52	0.78	9.04	113.43	116.54	0.30	30.0	32.9
0.53/L	0.030	1.73	-5.48	0.76	10.96	118.17	121.13	0.28	28.1	32.1
0.53/NL	0.030	1.73	-5.48	0.76	10.96	118.17	121.13	0.28	28.1	32.0
0.47/L	0.0307	1.76	-4.94	0.75	9.87	115.46	118.54	0.29	29.3	32.0
0.47/NL	0.0307	1.76	-4.94	0.75	9.87	115.46	118.53	0.29	29.2	32.5

The last two columns of Table 2 show the values of the developed torque $M_{t\varepsilon}$ and M_t. When calculating the first of them, the relevant parameter ε from Table 1 was applied. When calculating the torque M_t, the value $\varepsilon = 1$ was chosen for all solved cases. This last assumption can be questionable for larger initial extensions, as the fact that the spring is thermally shortened by length l_0 and not length l_m is neglected. As can be seen from Table 2, for small warming, the resulting thermomechanical force causes a small rotation of the rigid arms, and therefore the difference between the results of thermoelastic analyses according to the linear and nonlinear model is very small and differs only in other decimal places.

Therefore, to assess these differences, the results of the analyses at higher warming will be presented, when larger rotations of the rigid arm will occur. The solution was performed for elongation of springs Δl_m = 14.62 mm.

TABLE 3. Results of thermoelastic semianalytic analysis of torsional actuator for higher warming.

ΔT[°C]	50		60		70		80	
AT	L	NL	L	NL	L	NL	L	NL
φ°	8.59	8.69	10.27	10.45	11.94	12.22	13.59	14.00
$M_{t\varepsilon}$	140.49	139.55	168.59	166.94	196.69	194.05	224.79	220.04
M_t	160.06	159.00	190.25	188.33	224.07	221.18	256.09	251.59

As can be seen from Table 3, the difference between the results of the solution of the linear and nonlinear model is not significant. The way in which the parameter ε is taken into account has more significant effect on the torsional moment. It can be assumed that the application of heating to the elongated spring gives more reliable results. To verify the results of the solution by semianalytical models, a numerical model of the torsion actuator was created using the finite element method (FEM) with ANSYS [19]. The model was created using two LINK-type finite elements that replaced the springs, and perfectly rigid body elements, which modelled the rotating part of the T-shaped stiffer part. For rod finite elements of the LINK type, it is necessary to enter the thermal expansion α_T and the tensile stiffness ES with the modulus of elasticity E and with the cross-sectional area of the rod S. The effective tensile stiffness can be calculated from the spring constant k_m as $ES = k_m l_0$. The coefficient of thermal contraction can be determined from the temperature constant k_T: $\alpha_{Tm} = k_T/l_m$, because the heating is applied to the elongated spring by Δl_m. The second possibility is to set $\alpha_{T0} = k_T/l_0$, but these chose may be less acceptable. As our measurements showed, the nylon springs behave linearly even for large extensions (shortenings) [14]. A comparison of the results of the analytical methods and the linear finite element method is given in Table 4 for mechanical extension of springs for Δl_m = 14.62 mm. For the case α_{Tm}= 2.524e^{-3} [1/°C] and ES = 22.26 [N].

TABLE 4. Results comparison.

$\Delta \boldsymbol{T}$[°C]		10			50			80	
AT	**L**	**NL**	**Ansys**	**L**	**NL**	**Ansys**	**L**	**NL**	**Ansys**
φ^o	1.73	1.73	1.73	8.59	8.69	8.59	13.59	14.00	13.58
$M_{t\varepsilon}$	28.1	32.1	32.01	140.49	139.55	160.06	224.79	220.04	256.09
M_t	32.01	32.0		160.06	159.00		256.09	251.59	

As shown in the Table 4, an excellent agreement of the semianalytical and numerical results has been obtained for parameter $\varepsilon = 1$ for the linear models. In our further research, the semianalytical and numerical results will be evaluated by the measurement of real model of the torsion actuator.

6. CONCLUSIONS

The article presents the results of thermoelastic analysis of a torsional actuator, the action member of which is nylon artificial muscles with negative thermal expansion. A linear and nonlinear mathematical-physical model of a torsional actuator was constructed. The linear model is described by linear equations and is very simple in terms of application. The nonlinear model of the actuator is described by nonlinear equations that need to be solved numerically. Based on the geometric and thermomechanical parameters of the actuator, its thermoelastic semianalytical analyses were performed, the results of which are action variables such as the angle of rotation of the actuator arms and the action torque. The results of the analyses show that the action variables increase with increasing heating of one of the two nylon springs. Due to the experimentally determined linearity of the behaviour of nylon springs, the difference in the results is small for real warming up to 50°C. At higher warmings, which are, however, limited from a practical point of view, the results of the solution of the linear and nonlinear model differ significantly. To verify the results of the solution, a computational model of the actuator in the environment of the ANSYS finite element method software [19] was compiled. From the comparison of the results it can be stated a very good agreement of the solution obtained by the analytical and numerical method. Analytical models of the solution will be used in further research for automatic control and management of the torsion actuator. In our future work, the calculation results will be verified by experimental measurements on the physical model of the actuator.

ACKNOWLEDGEMENT

The authors gratefully acknowledge financial support by the Research and Development Agency under Contract No. APVV-19-0406, and VEGA 1/0102/18.

REFERENCES

1. CS. Haines *et al.,* "Artificial Muscles from Fishing Line and Sewing Thread"*,* Science **343**, 868-872 (2014), ISSN 1095-9203.
2. P. Zhang, G. Li, "Healing-on-demand composites based on polymer artificial muscle"*,* Polymer **64**, 29-38 (2015), ISSN: 0032-3861.
3. SH. Kim *et al.,* "Harvesting temperature fluctuations as electrical energy using torsional and tensile polymer muscles", Energy and Environment Science **15**, (2015), ISSN 1754-5692.
4. A. Cherubini, G. Moretti, R. Vertechy, M. Fontana, "Experimental characterization of thermally-activated artificial muscles based on coiled nylon fishing lines", AIP Advances **5**, (2015), ISSN 2158-3226.
5. TF. Otero, JG. Martinez, "Physical and chemical awareness from sensing polymeric artificial muscles. Experiments and modelling", Progress in Polymer Science **44**, (2015), ISSN 0079-6700.

6. S. Sharafi, G. Li, “A multiscale approach for modeling actuation response of polymeric artificial muscles”, Soft Matter **19**, (2015), ISSN 3833-3843.
7. S. Kianzad *et al.,* “Nylon coil actuator operating temperature range and stiffness”*,* in *Electroactive Polymer Actuators and Devices 2015*, Proceedings SPIE 9430, edited by Y. Bar-Cohen (SPIE, Bellingham, WA, 2015).
8. S. Kianzad *et al.,* “Variable stiffness structure using nylon actuators arranged in a pennate muscle configuration”, in *Electroactive Polymer Actuators and Devices 2015*, Proceedings SPIE 9430, edited by Y. Bar-Cohen (SPIE, Bellingham, WA, 2015).
9. G. Moretti, A. Cherubini, R. Vertechy, M. Fontana, “Experimental characterization of a new class of polymeric-wire coiled transducers”, in *Behaviour and Mechanics of Multifunctional Materials and Composites 2015,* Proceedings SPIE 9432, edited by NC. Goulbourne (SPIE, Bellingham, WA, 2015).
10. L. Wu *et al.,* “Nylon-muscle-actuated robotic finger”, in *Active and Passive Smart Structures and Integrated Systems 2015,* Proceedings SPIE 9431, edited by Wei-Hsin Liao (SPIE, Bellingham, WA, 2015).
11. P. Zhang *et al.*, “Healing of polymeric artificial muscle reinforced ionomer composite by resistive heating”*,* Journal of Applied Polymer Science **133**, (2016), ISSN 1097-4628.
12. Q. Yang, G. Li, “A top-down multi-scale modeling for actuation response of polymeric artificial muscles”*,* Journal of the Mechanics and Physics of Solids **92**, (2016), ISSN 0022-5096.
13. Chia-Yu Chen *et al.,* “Motion Guidance Sleeve: Guiding the Forearm Rotation through External Artificial Muscles”, in *CHI´16*, Proceedings of the 2016 CHI Conference on Human Factors in Computing Systems 2016, (Association for Computing Machinery, NY, United States, 2016), pp. 3272–3276. ISBN 978-1-4503-3362-7.
14. J. Murín, V. Goga, J. Hrabovský, D. Búc, P. Podešva, “Measurement and numerical analysis of the artificial muscles made of fishing line”*,* Advanced Materials Letters **8**, pp. 635-640, (2017), VBRI Press, ISSN 0976-3961. DOI: 10.5185/amlett.2017.7105.
15. M. Minár, V. Goga, R. Čapková, K. Ondrejička, J. Murín, “Basic parameters of coiled fishing line actuator”, in *K&I 2020*, Proceedings of the 30th International Conference on Cybernetics and Informatics, eddied by J. Cigánek, Š. Kozák, A Kozáková. (Piscataway, New Jersey, 2020), pp. 204-208. DOI: 10.1109/KI48306.2020. 9039870.
16. J. Murín, V. Goga, J. Hrabovský, P. Podešva, R. Gogola, “Numerical analysis of the artificial muscle made of fishing line”, in *APCOM 2016*, Proceedings of 22nd international conference on applied physics of condensed matter, edited by J. Vajda, I. Jamnický (STU v Bratislave, Slovakia, 2016), pp. 231-235. ISBN 978-80-227-4572-7.
17. M. Minár, V. Goga, J. Murín, “The main features of coiled fishing line actuator”, in *ELITECH´20* [electronic source], 22nd Conference of doctoral students. (Spektrum STU, Bratislava, Slovakia, 2020), ISBN 978-80-227-5001-1.
18. Wolfram MATHEMATICA 9.0.1.0. Wolfram Research, 2013.
19. ANSYS Swanson Analysis System, Inc., 201 Johnson Road, Houston, PA15342/1300, USA.